AIAA JOURNAL
Vol. 41, No. 12, December 2003

Examining the Effect of Flow Reversal on Seven-Hole Probe Measurements

A. J. Pisasale* and N. A. Ahmed†
University of New South Wales, Sydney, New South Wales 2052, Australia

Multihole pressure probes are frequently used to gather flow data, sometimes in highly three-dimensional flow. If the flow is reversed, no method currently exists for determining whether the multihole probe is facing the right direction for data acquisition, and that the flow is as such. A seven-hole probe is rotated in yaw by 360 deg, and rules are formulated to determine if a seven-hole probe is in a reversed flow. The current study allows seven-hole probes to be used for gathering data in steady reversed flows and gives an indication whether a pressure probe is insufficient for the measurement instrument, as in the case of highly recirculating unsteady turbulent flows. An application of the technique thus developed is also given.

Nomenclature

A, B, C, D	=	generalized constants
Cp_i	=	pressure coefficient at port i
H	=	step height
n	=	total number of ports
$\hat{P}_{jk\ldots m}$	=	average pressure over ports $jk\ldots m$
P_s	=	static pressure in the freestream
$P_s/Q_{\inf}$	=	static pressure nondimensionalized with freestream q
P_T	=	total pressure of the flow
$P_{1,2,\ldots,m}$	=	measured pressure from each of the pressure ports
q	=	dynamic pressure of the flow
U	=	magnitude of flow velocity
W	=	ordinate defined for second rule
$X/H, Y/H$	=	ordinates defining nondimensional length and height
Y	=	ordinate defined for first rule
α	=	pitch angle, deg
β	=	yaw angle, deg
ΔP_i	=	recorded differential pressure from port i
ΔP_T	=	recorded differential total pressure
ϵ_i	=	error at port i
ϵ_T	=	total error
θ	=	flow dihedral angle, deg
ρ	=	density of ambient air
ϕ	=	flow azimuthal angle, deg

I. Introduction

MULTIHOLE pressure probes are often used to conduct simple flow surveys. Given their prolific use, it is surprising to discover that there still remains many aspects of their performance that have not been thoroughly researched. For instance, if a seven-hole probe is unknowingly inserted into a recirculating flow, or simply a flow of angularity beyond the probes calibration range, no method currently exists to determine from the measured pressures that the flow is not within the calibration region. Consequently, it is feasible that pressure probes are being used incorrectly because flow properties are being calculated under the false assumption that the probe is within the calibration range. Even within the calibration region, there exists questions of the calibration's Reynolds-number dependence.[1]

Recent works[2,3] have also demonstrated that nondimensionalization of calibration coefficients used in existing multihole probe theory suffers from a singularity problem and that the mathematics used to calibrate and determine flow properties might, in some cases, need revision, particularly for flows with high angularity. In spite of this improvement, if the probe is inserted into a region of reversed flow, where the velocity vector is pointing away from the direction to which the probe is designed to measure so that the probe tip is in the wake of the flow, problems will incur.

Such a flow might be encountered as a result of recirculation, say, for example, behind a cylinder. As most common calibration methods are only valid for flows toward the probe tip within a cone of approximately 75 deg aligned with the probe,[4–7] resolution of velocity components and total and static pressure from the measured probe pressures would be erroneous, if the probe were in a steady reversed flow.

Pressure probes have seemingly been used in the past to examine flows appearing to contain recirculation.[5,7] In these cases flow is examined around a hemispherical cylinder and an ogive-cylinder, respectively. However, in both of these cases the flowfields given are in a plane perpendicular to the main flow, which is also shown in the corresponding detailed flow studies.[8,9] Consequently, the flow is within the probe's calibration region and does not represent a reversed flow.

Recirculating flows have nonetheless been investigated using a five-hole probe.[10] However, in a related study,[11] where the use of the probe is described in detail, it is revealed that at each test point the probe is first nulled in the yaw direction. Assuming the probe was nulled correctly, which will be examined further later, the probe tip will be pointing into the flow, and a correct measurement of the flow can be made.

Flow reversal caused by a backward-facing step, was also investigated by Rediniotis and Kinser,[12] who used it as a test case for an almost omnidirectional probe. The present work, however, focuses on the effects of flow reversal on more common seven-hole probes and the correct use of these in an unknown flow.

If the pressure probe is to be used in a nonnulling manner, some generic rules would be desirable in order to determine when the probe is in a reversed flow, and consequently if it needs to be rotated and to what extent.

Simple rules have been used in the past to test for validation of data[7] by checking that the central hole is within a tolerance of the leeside holes. However, this rule does not determine the extent to which the probe is out of range.

Thus, the purpose of this study is to develop such rules, which can be applied in a preprocessing manner, to the probe pressure

Received 5 October 2002; revision received 5 June 2003; accepted for publication 8 August 2003.

*Ph.D. Candidate in Aerodynamics. Member AIAA.
†Senior Lecturer, Aerospace Engineering.

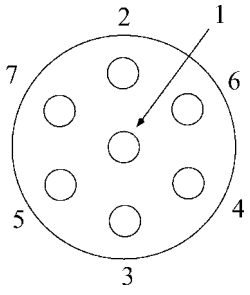

Fig. 1 Illustration of the port numbering of the seven-hole probe.

data to determine the validity of the data to correctly determine flow properties, or whether the probe requires rotation from its original setup to do so. A brief investigation of Reynolds effect on probe performance is also conducted, and an application of the method is given.

II. Description of Experiment

A seven-hole "cobra" probe from the Aeroprobe Corporation was calibrated in the 18 × 18 in. (0.457 × 0.457 m) subsonic wind tunnel of the University of New South Wales aerodynamics laboratory. The probe was placed in a mounting fixed to the roof of the tunnel that could rotate the probe though pitch and yaw angles. A bank of Honeywell pressure transducers and an FCO510 manometer from Furness Controls, Ltd., recorded the pressures from each of the seven pressure ports and the total pressure from a pitot-static tube, respectively, at each measurement point. The static pressure from the pitot-static tube was also subtracted from all pressure readings[9] to give values at each pressure port i of ΔP_i, as well as ΔP_T, and a schematic of the port numbering is given in Fig. 1. Nondimensional pressure coefficients Cp_i can be formed by dividing the recorded gauge pressure with the dynamic pressure; therefore,

$$Cp_i = (P_i - P_s)/q = \Delta P_i/\Delta P_T \tag{1}$$

The bank of transducers has a stated resolution of ±0.25%FS (±3.1 Pa) but are calibrated before each experiment to improve the accuracy of the pressure readings, and the ambient air pressure and temperature were periodically checked to account for any changes in air density. The probe was rotated a full 360 deg in yaw at 10-deg increments for the three pitch values of −20, +20, and 0 deg. Unfortunately, the physical constraints of the mechanism did not allow for full 360-deg rotation in pitch.

The experiment was repeated twice for a total of three sets of data at the freestream velocity of 15 m s^{-1}. It was also repeated at the higher and lower speeds of 20 and 10 m s^{-1}, respectively, to examine the effect of Reynolds number on probe performance. The average repeatability was within ±1.85%, excluding data points near zero.

III. Formulation of Generic Rules

A. Very High Wake Angles

The nondimensional pressure coefficients are plotted in Fig. 2 for the full range of yaw angles at zero pitch. It can be seen that in the ranges $\beta > 125$ deg, $\beta < -125$ deg all pressure ports record approximately the same values. The same trend is also noted at both positive and negative pitch locations in Figs. 3 and 4, respectively. The plot of calibration data at zero pitch, shown in Fig. 2, is similar to that of Zilliac's[7] for the calibration region.

Therefore, it appears that if all of the recorded pressures are approximately of the same value then the probe tip should be rotated 180 deg in yaw. It is necessary to note, however, that, although we are dealing with relationships between recorded pressure differences, these relationships are also generally true for pressure coefficients and absolute pressures. For instance, if $\Delta P_1 > \Delta P_2$, then $Cp_1 > Cp_2$, and consequently $P_1 > P_2$.

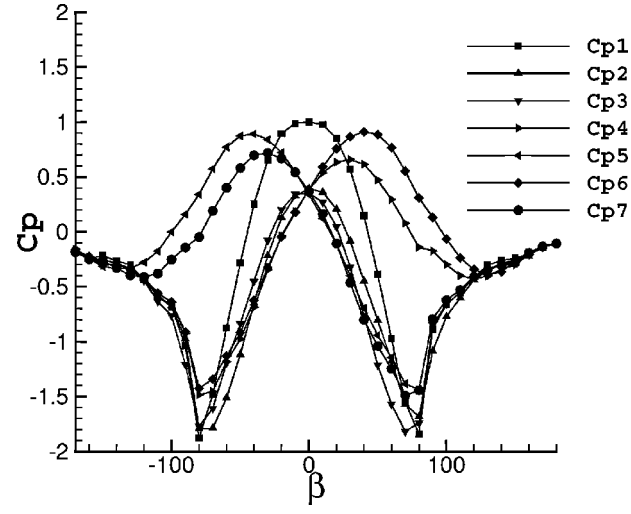

Fig. 2 Plot of pressure coefficients Cp_i for all ports at zero pitch and for ±180 deg in yaw.

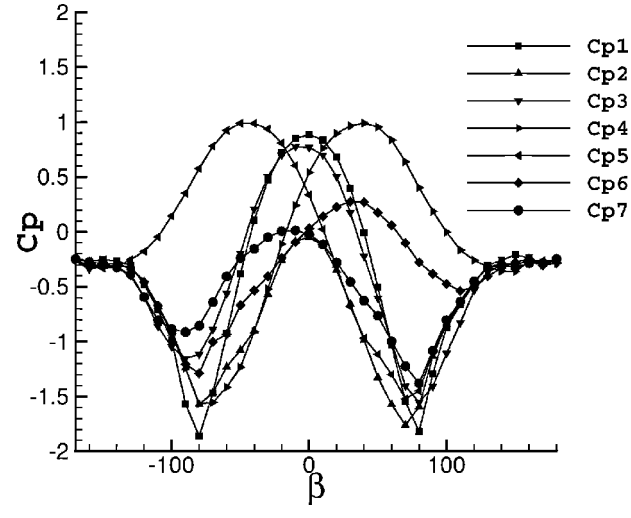

Fig. 3 Plot of pressure coefficients Cp_i for all ports at +20 deg pitch and for ±180 deg in yaw.

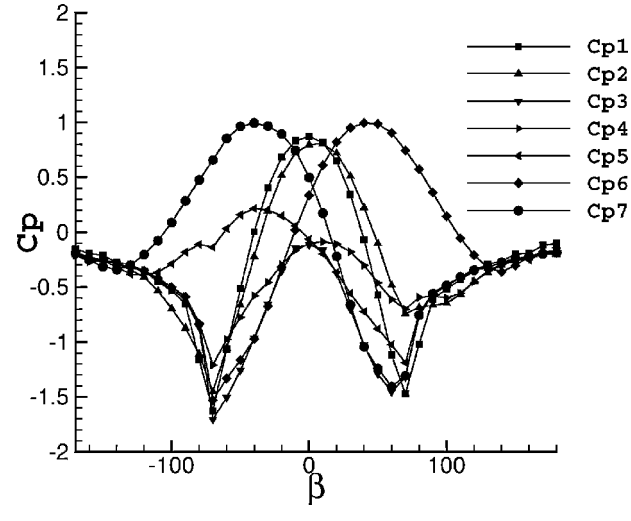

Fig. 4 Plot of pressure coefficients Cp_i for all ports at −20 deg pitch and for ±180 deg in yaw.

A new constant $\hat{P}_{jk\ldots m}$ to be the mean pressure of the indices specified is now introduced. For example,

$$\hat{P}_{1346} = (P_1 + P_3 + P_4 + P_6)/4 \tag{2}$$

This new, generic definition is employed first to distinguish it from other mean operations, such as $\bar{P}$ (Ref. 13), and second, because a generalized notation will be required later.

The first rule can now be formulated. Because all ports record the same pressure, it is likely that all pressure ports are in stalled flow or wake in the regions $\beta > 125$ deg and $\beta < -125$ deg. If any pressure port is not in this same flow, then the probe is not in this region.

The percentage error between a pressure port i and a specific mean quantity is obtained as such:

$$\epsilon_i = |(\hat{P} - P_i)/\hat{P} \times 100| \tag{3}$$

and the total error[14] is determined as

$$\epsilon_T = \sqrt{\epsilon_1^2 + \epsilon_2^2 + \cdots + \epsilon_n^2} \tag{4}$$

where n denotes the total number of ports.

For the specification of this first rule, $\hat{P}_{1234567}$ is first calculated, then the error using this definition of $\hat{P}$ is found for each port, using Eq. (3). Finally, the total error over all ports ($n = 7$) is calculated using Eq. (4), and Y is set equal to this total error to give

$$Y = (100/\hat{P}_{1234567})\left[\sum_{i=1}^{7}(\hat{P}_{1234567} - P_i)^2\right]^{\frac{1}{2}} \tag{5}$$

However, the problem with this equation is that if pressure coefficients are substituted using Eq. (1) it can be shown that the equation relies on a prior knowledge of the static pressure, which is often not known in an unknown flow. This gives insight into why equations in pressure probe theory are typically expressed in the form

$$Y = (A - B)/(C - D) \tag{6}$$

where the constants A, B, C, and D can be substituted for recorded pressures, pressure coefficients, or absolute pressures, to give exactly the same value of Y at that point. For example,

$$Y = \frac{\Delta P_2 - \Delta P_3}{\Delta P_4 - \Delta P_5} = \frac{Cp_2 - Cp_3}{Cp_4 - Cp_5} = \frac{P_2 - P_3}{P_4 - P_5} \tag{7}$$

Clearly, the equation for Y must be of this form to be nondimensional. However, in the region of interest, all of the pressures are approximately the same. Although this is an advantage in terms of the numerator, causing the total error to be lowered [Eq. (4)] in order to nondimensionalize the equation, a denominator must also be specified. It seems likely that all combinations of denominator will also be zero in this region. Consequently, the Y ordinate will be undefined in the region of most interest.

This actually poses quite a dilemma. To proceed, it was decided to nondimensionalize with the dynamic pressure q and to define the Y ordinate as

$$Y = (100/q)\left[\sum_{i=1}^{7}(\hat{P}_{1234567} - P_i)^2\right]^{\frac{1}{2}} \tag{8}$$

which can be expressed in terms of recorded pressures by substituting directly for corresponding terms, or in terms of pressure coefficients as

$$Y = 100\left[\sum_{i=1}^{7}(C\hat{p}_{1234567} - C_i)^2\right]^{\frac{1}{2}} \tag{9}$$

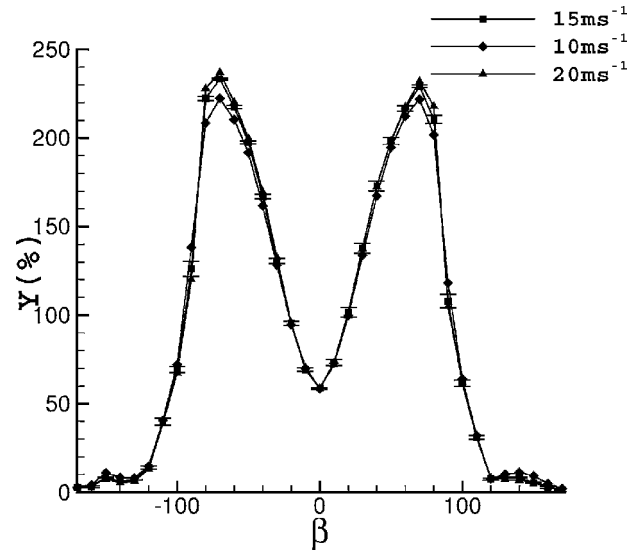

Fig. 5 Plot of Y for ±180 deg yaw for zero pitch at 15, 10, and 20 m s^{-1} with errors shown.

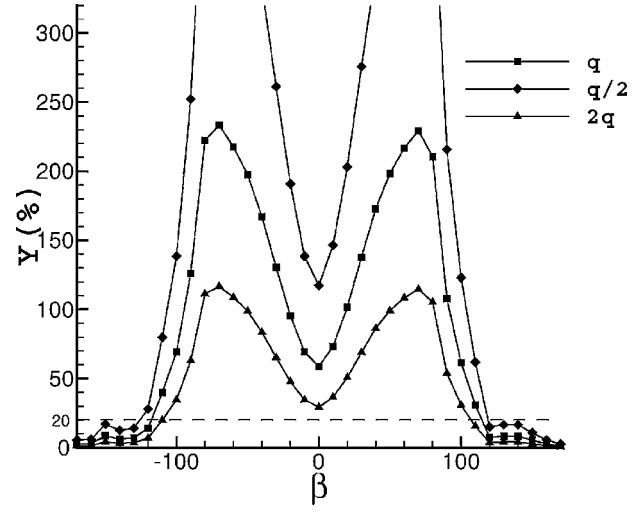

Fig. 6 Plot of Y for ±180 deg yaw for zero pitch at 15 m s^{-1}, with rescaled estimates of dynamic pressure.

This equation is plotted against yaw angle, for the three speeds tested, in Fig. 5, which also demonstrates that the relationship is mostly Reynolds-number independent over this velocity range.

It is perhaps noteworthy at this stage to reflect on the application of this method. First, as the probe is physically quite symmetrical, geometrically consisting of a cone-cylinder, the relationship demonstrated in Fig. 5 should also be true if the yaw angle were substituted for the pitch angle α or dihedral angle θ in polar coordinates, for at least the very high wake angles. The reasoning for this is that if the probe is rotated 180 deg in either of these alternate coordinates it would physically be in the same position as that demonstrated by a rotation in yaw (Fig. 5). In this way, although the rule has been demonstrated for yaw, it is also more generally applicable.

Second, use has been made of the local dynamic pressure to nondimensionalize the Y ordinate in Fig. 5, which is of course unknown when the probe is used in flow studies. As already mentioned, it is extremely difficult to nondimensionalize using measured port pressures, and doing such will result in an undefined function in the region of investigation. The dynamic pressure in this case is simply a method of scaling the Y axis. To make use of Eqs. (8) or (9), it is thus necessary to make an approximate guess of the local dynamic pressure of the unknown flow. Illustrated in Fig. 6 is the effect of doubling or halving the dynamic pressure on the data obtained at 15 m s^{-1}.

Investigation can now proceed by setting a limit of, say, 20%, under which the probe needs to be rotated 180 deg. This will exclude data points where $|\beta| > 130$ deg (or alternatively α or θ can be substituted for β).

The procedure to be followed in sequence is now summarized as follows. Port pressures are recorded from the probe, q is estimated, and Y is calculated from Eq. (8). If the value of Y is less than 20%, then the probe is rotated by 180 deg. Assuming that the dynamic pressure estimate is within half or double of the actual local dynamic pressure, the method is shown to be viable (Fig. 6).

The curious reader might wonder why a simple investigation of whether all of the pressure ports record the same value should not suffice as a rule, instead of the method just outlined. However, when dealing with real experimental data, it is unlikely that all pressure ports will ever record exactly the same value. The slight differences in pressure might either be as the result of a reversed flow, or of a nonreversed flow. It would be impossible to tell which of the preceding two is the actual one, without some knowledge of the scale of the pressure differences. Use has been made of a guessed dynamic pressure in Eqs. (8) and (9) to scale the results.

If the scale of the measured pressures was intuitively known, say, for instance, by knowing some flow property of the unknown flow, then simply examining the pressures might be sufficient, as the experimenter would have an idea of the scale of the differences to look for in the recorded data. However, this is essentially the same as guessing the dynamic pressure, and using Eqs. (8) and (9) on the recorded data to determine the scale of the differences. Thus, both methods are actually the same, with Eqs. (8) and (9) being merely a more formal description.

B. Intermediate Angles

As mentioned earlier, the calibration region is established as $|\beta| < 75$ deg, and the rule developed in the preceding section applies to angles $|\beta| > 130$ deg. A second rule is now developed, which will be applicable in the intermediate angle region $75 \text{ deg} < |\beta| < 130$ deg. Referring back to Figs. 2–4, physically at least one of the probe's pressure ports remains in the higher pressure side of the flow, where it reaches a maximum, probably when the port surface is perpendicular to the flow, and then falls away to the same constant value of the other pressure ports as the yaw angle is further increased. The four ports opposite this maximum pressure port, on the other hand, are already in stalled flow, and so record approximately the same pressure.

For example, referring to Fig. 2, in the range $30 \text{ deg} < \beta < 130$ deg, the port with the maximum pressure is six, thus, for this case $P_{\max} = P_6$. Using Fig. 1 for identification of the port locations, the average pressure can be calculated over ports 1, 3, 5, and 7, as these are the ports that will stall in the region under investigation. This will give

$$\hat{P}_{1357} = (P_1 + P_3 + P_5 + P_7)/4 \tag{10}$$

In a similar manner to the first rule developed for very high wake angles, the sum of errors between these ports and their average can be found. However, unlike the first rule, nondimensionalization using the port pressures is now possible. To generalize the expression, the subscript on $\hat{P}$ is changed to j, k, l, m (instead of 1, 3, 5, 7), $P_{\max}$ is used instead of P_6, and the summation is over the four indices j, k, l, m only. The new ordinate is also denoted by W instead of Y to distinguish it from the preceding rule and is thus defined as

$$W = \frac{100}{(P_{\max} - \hat{P}_{jklm})}\left[\sum_{i=j,k,l,m} (\hat{P}_{jklm} - P_i)^2\right]^{\frac{1}{2}} \tag{11}$$

Here, as before for Y, the yaw angle β could be exchanged for the pitch angle α, or dihedral angle θ, because of the symmetry of the probe. Thus, as another example, by referring to Fig. 3, for intermediate yaw angles of $-130 < \beta < -30$ the maximum pressure is recorded at port 5, and from Fig. 1, $\hat{P}$ is averaged over ports 1, 2, 4, and 6. The final equation for W is then

$$W = [100/(P_5 - \hat{P}_{1246})]\left[(\hat{P}_{1246} - P_1)^2 + (\hat{P}_{1246} - P_2)^2 + (\hat{P}_{1246} - P_4)^2 + (\hat{P}_{1246} - P_6)^2\right]^{\frac{1}{2}} \tag{12}$$

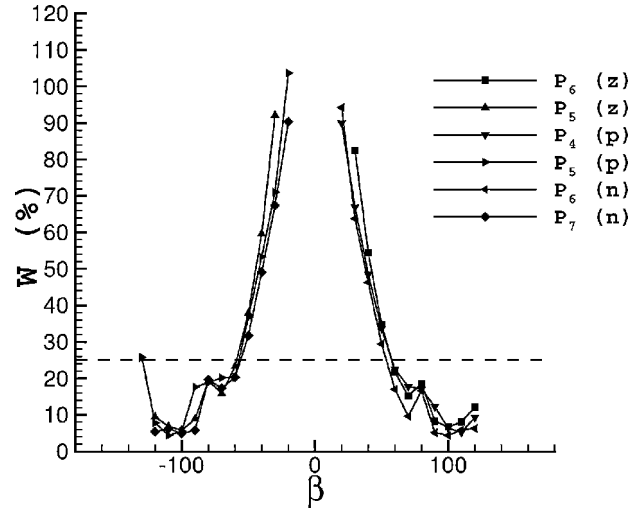

Fig. 7 Plot of W for all of the pressure data obtained at 15 m s^{-1} for the port with the maximum pressure at zero (z), positive (p), and negative (n) pitch.

To further illustrate this point, the method is applied to all of the data collected at 15 m s^{-1}, including both positive and negative pitch angles, and plotted in Fig. 7. It can be seen that the graph follows the same trend, reducing to a minimum in the region of interest. The figure only shows W, where the maximum pressure comes from the same port. For instance, in the first example considered, P_6 was maximum; however, as the probe was rotated further, P_1 becomes maximum. Thus, the graph is only shown for the region where P_6 is maximum. As P_1 takes over as the maximum port pressure again, it does so only marginally. In fact, P_1 is only slightly greater than P_6, as all the pressure ports record approximately the same value. Referring back to Fig. 7, this clearly corresponds to the region of the first rule, to which Y was devised.

Consequently, as shown by P_5 in Fig. 7 at 130 deg, the function W will begin to increase again in the wake region described in the first rule, as all of the pressures become approximately equal and W becomes undefined. This is not actually a problem because if the first rule is applied correctly before this second rule then the probe will be known to be in flow within $-130 \text{ deg} < \beta < 130$ deg. Such undefined values of W will, of course, then be excluded.

Examining Fig. 7, a threshold can be set, say of 25%, which will define whether the probe needs rotating. If the probe does require rotation, it can then be rotated 90 deg in the direction indicated by the maximum port pressure $P_{\max}$ towards P_1 as shown in Fig. 1. For instance, if port 2 is the maximum and W indicates that rotation is required, then the probe is rotated in a plane to which ports 2 and 1 are aligned (in this case the pitch plane) in the direction towards the flow, which would be the direction required to make P_1 maximum (positive pitch).

The entire procedure for preprocessing of the measured pressure, for all angles, has been outlined in a flowchart in Fig. 8.

IV. Examination of the Effect of Reynolds Number

It is perhaps an opportune moment to briefly examine the effect of Reynolds number on the calibration, given that data have been collected for a much greater range of yaw angles than is traditional. Referring to Figs. 9–15, the calibration data collected at zero pitch are shown for the three speeds tested, and error bars are shown for the repeated data. The Reynolds number is calculated based on the probe-tip diameter.

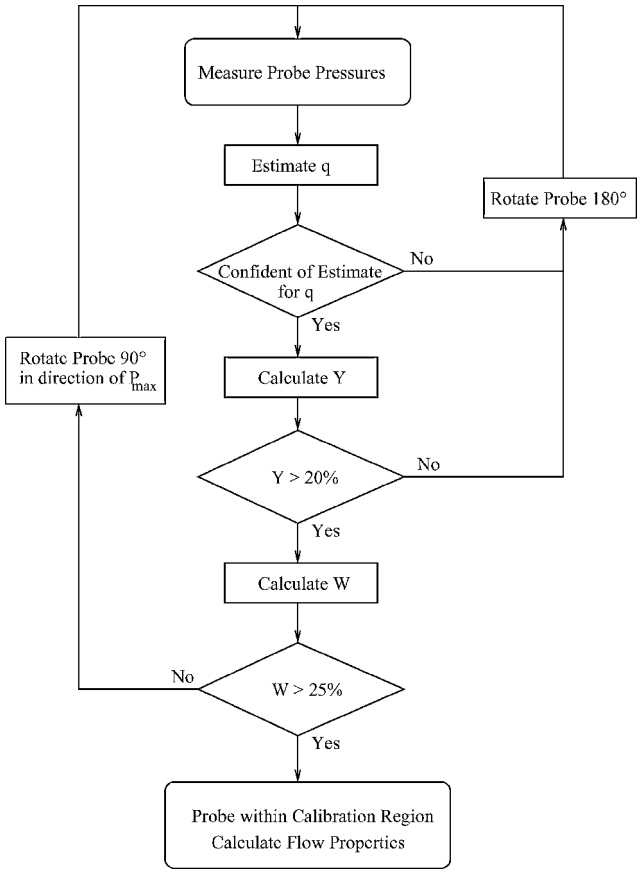

Fig. 8 Flowchart of the preprocessing procedure applied to measured pressured of the probe.

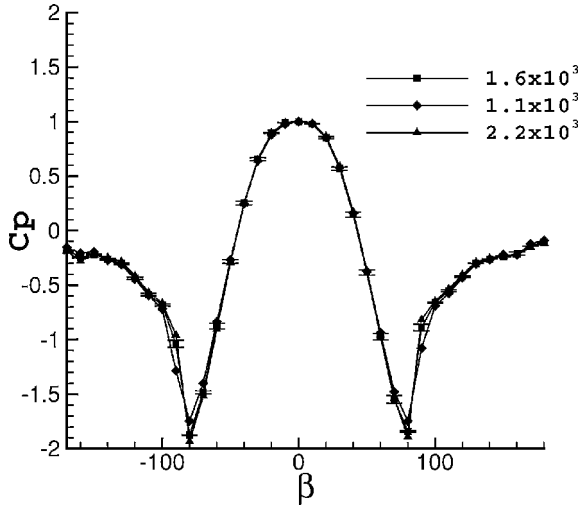

Fig. 9 Plot of *Cp*1 against yaw angle for different Reynolds numbers with errors shown.

Surprisingly, there appears to be very little Reynolds-number effect when the probe tip is in the wake, corresponding to $|\beta| > 130$ deg. There is also very little effect for the higher intermediate angles corresponding to $|\beta| > 90$ deg. In fact, the region appearing to have the highest Reynolds-number effect, and also the largest variation in repeatability, is for high angles within, and just outside, the calibration range, corresponding to approximately $30 < |\beta| < 90$ deg. However, given that the range of Reynolds number tested is small and the overlap in repeatability at some points, it cannot be said conclusively that there is obvious Reynolds-number effect. However, some effect is indicated.

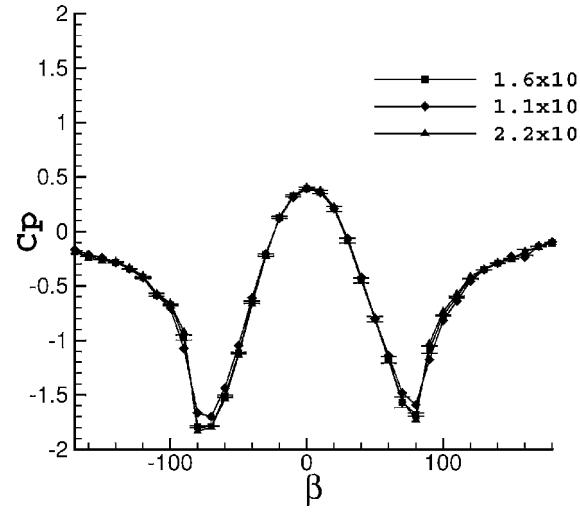

Fig. 10 Plot of *Cp*2 against yaw angle for different Reynolds numbers with errors shown.

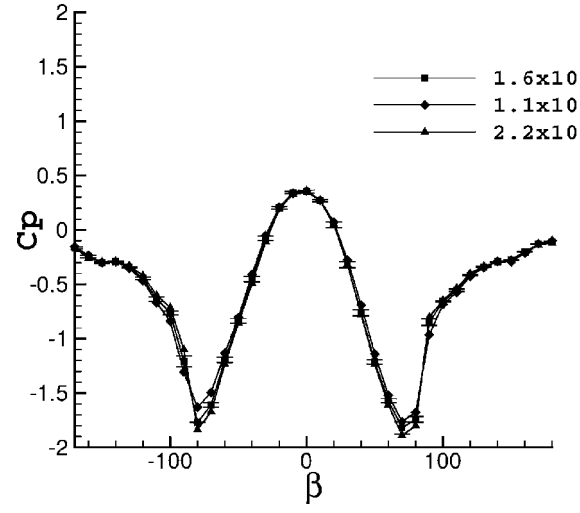

Fig. 11 Plot of *Cp*3 against yaw angle for different Reynolds numbers with errors shown.

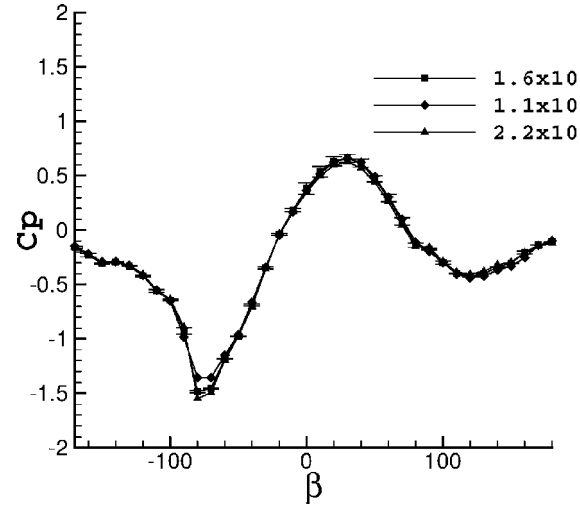

Fig. 12 Plot of *Cp*4 against yaw angle for different Reynolds numbers with errors shown.

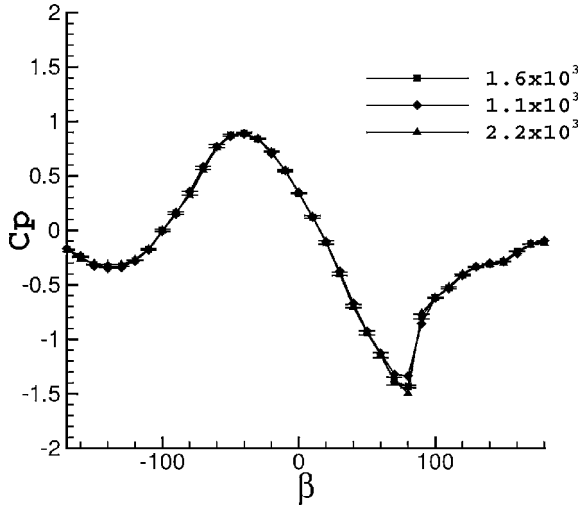

Fig. 13 Plot of *Cp*5 against yaw angle for different Reynolds numbers with errors shown.

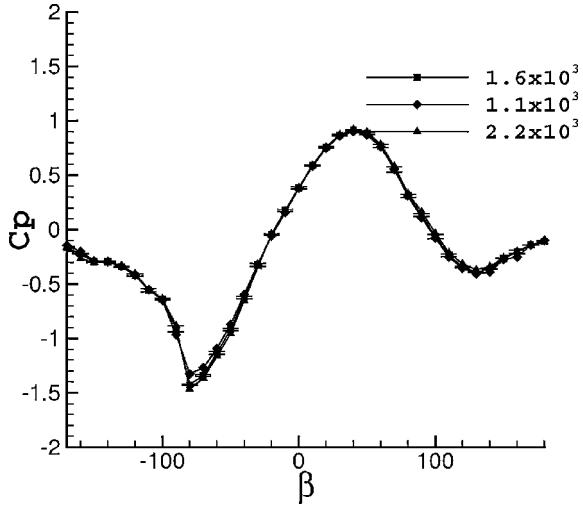

Fig. 14 Plot of *Cp*6 against yaw angle for different Reynolds numbers with errors shown.

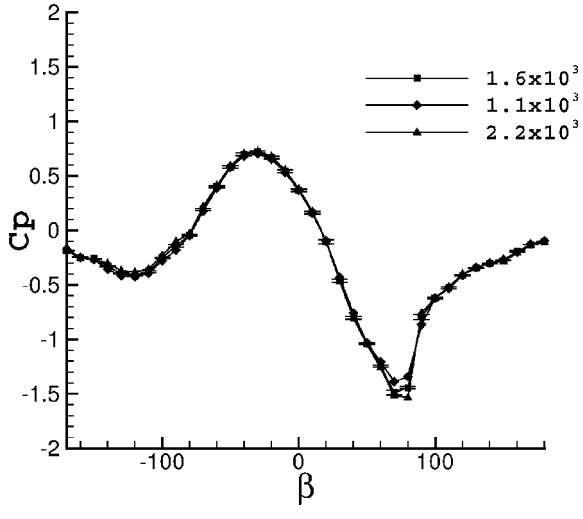

Fig. 15 Plot of *Cp*7 against yaw angle for different Reynolds numbers with errors shown.

Reynolds-number effect on pressure probes has been noted before.[1,15,16] Dominy and Hodson[1] suggested that a recirculation bubble might be present, which contributes to this effect. Given that the probe used here is geometrically very similar, the recirculation bubble might also be present here.

This will perhaps aid in explaining the unusual results of Figs. 9–15. For the angles within the calibration region, the recirculation bubble over the cone tip would make the results Reynolds-number dependent,[1] as the data appear to indicate. As the yaw angle is increased past 90 deg, however, this recirculation bubble is diffused and swept away by the flow, which might explain the reduced effect in the intermediate angles. At very high angles, when the probe tip is in the wake, the conical tip effectively streamlines the probe, minimizing the Reynolds-number effect.

Unusually, there should be some Reynolds-number effect in the intermediate and very high angle regions as a result of the nonlinear, viscous effects of the wake. Albeit, the examination given here is admittedly only over a very short Reynolds-number range, and these effects might be found in a more extensive examination.

It is nonetheless important to realize that the Reynolds-number effect noted here is more significant in the calibration region than the other regions. However, as only five of the seven holes are required for measurement, this effect will be minimal in the calibration region as the holes in stalled flow are not used. It has been suggested[16] that the Reynolds number can be taken into account by calibrating the probe over a range of Reynolds number. As the Reynolds number of the flow local to the probe is typically unknown, converting probe data into flow properties might then require use of an iterative method.

Examining further Figs. 9–15, and also Fig. 2, there is very little change in the functional form of the data between $\beta = 50$ and 90 deg, at zero pitch. This indirectly implies that if Reynolds number could be taken into account in the calibration, then this probe could be used up to dihedral angles θ just below 90 deg, which would extend the calibration range of 75 deg stated earlier.

V. Experimental Application to Flow over a Step

To demonstrate the method, it is applied to flow over a backward-facing step. A step is constructed with a 5.7-in. (0.145-m) height H and 900-mm width and placed in the open-jet wind tunnel of the University of New South Wales; a description of which can be found in Refs. 17–19. The step height was chosen to correspond with a similar experiment.[12] The experiment, however, could not be performed at the same Reynolds number because of wind-tunnel restrictions, but was performed at the Reynolds number of 0.31×10^6, which corresponds to a freestream velocity of 33 m/s, the maximum speed at which this wind tunnel can be operated.

As the step contains no roof or side panels, it should not be thought of in the traditional sense as a backward-facing step, but it should be nonetheless sufficient to demonstrate this method. The test was performed by orienting the probe in the four different directions of front, back, up, and down at each measurement point. Pressure data were acquired from the probe using the same bank of Honeywell transducers mentioned earlier and averaged over a 10-s period, while the FCO510 manometer recorded the freestream dynamic pressure. Each probe orientation was tested at each point of a two-dimensional mesh of $8H$ length and $1.4H$ height. The data from the four orientations, shown in Table 1, could then be examined concurrently to determine the correct orientation before postprocessing the pressure data to obtain flow properties.

The dynamic pressure q was estimated by the difference between the maximum pressure and the average of the remaining pressures. For flow in the central zone, this equals $P_1 - \bar{P}$, which is a common traditional definition. An important simplification can be made by assuming that the flow is steady at a given point; the validity of this assumption will be examined in more detail later. Therefore, the dynamic pressure will be constant for all orientations. After finding an estimate for the dynamic pressure at each orientation, the final estimate is taken as the maximum of these values. The maximum is taken, as it has been shown that this pseudodynamic pressure is more likely to be an underestimate of the actual dynamic pressure.[2]

Table 1 Method applied to data at all four orientations, along with the functions *Y* (%), *W* (%), and the port number with the corresponding maximum pressure

	Front			Back			Up			Down		
q estimate	Y	W	No.	Y	W	No.	Y	W	No.	Y	W	No.
2.6	105	29	3	55	68	7	111	23	3	84	18	3
2.8	83	203	2	43	123	4	123	16	6	107	42	5
10.4	33	8	3	96	17	3	37	9	3	51	10	3
4.3	84	7	3	53	21	3	89	13	3	96	12	3
60.7	47	——	1	5	——	1	119	6	6	62	18	7
44.0	86	——	1	8	——	1	136	4	6	110	14	5

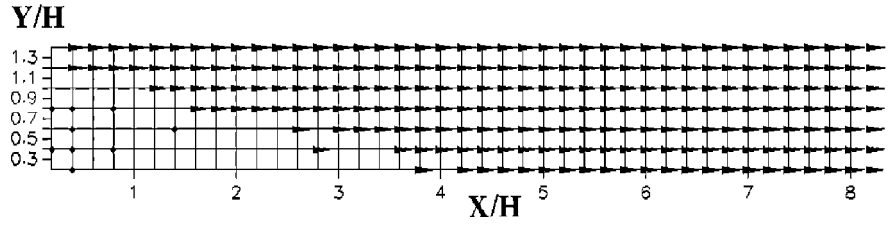

Fig. 16 Plot of the flow showing only orientations. The points in the bottom left are out of the page.

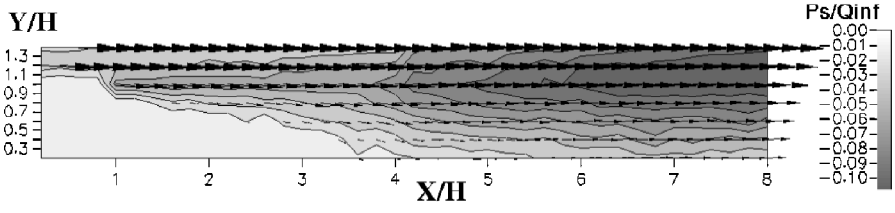

Fig. 17 Final flowfield showing vectors superimposed onto the static pressure. The pressure and velocity of inconclusive points are set to zero.

The thresholds indicating reorientation are set at 20% for Y and 25% for W. The probe was inserted into the flow from the right side, looking downstream, for all orientations. This means that when the probe is in the front orientation the hole numbering is for Fig. 1 rotated 90 deg clockwise, with holes 5 and 7 facing the top and holes 4 and 6 facing the bottom.

Examining the first data point in Table 1, none of the Y values indicate a rotation of 180 deg. As all four orientations use the same estimate for q, they can all be compared in relation to each other. Thus, if the estimate for q was increased the Y value in the back orientation will pass the threshold before the Y value in the front orientation, implying that the front direction is correct.

However, the W values suggest that this data point is inconclusive. In both the up and down orientations port 3 is the maximum; however, in the back orientation the maximum is port 7, which, neglecting the streamwise component, is in a different direction. It should, however, be remembered that as some of the orientations might be pointing with the probe tip in the wake, the port with the maximum pressure does not necessarily indicate that the flow is coming from that direction. Equally important is that W is independent of the estimate for q, and, consequently, W values are independent of each other. The second point is also inconclusive for similar arguments.

The third and fourth points however appear to suggest that the flow is toward port 3, which remains on the same side when the probe is rotated through the different orientations. This indicates that the flow is perpendicular to the plane of measurement and is consequently three-dimensional.

The last two points appear to show quite conclusively that the front orientation is correct. In the front orientation Y indicates no need for rotation. In the back orientation Y indicates rotation to the front position. In the up and down orientations W suggests rotation to the front position. It is not necessary to calculate W when the maximum pressure is recorded from the central hole, as this will occur only when the probe is aligned into the flow or 180 deg away from the flow.

In this manner a map of correct orientations can be developed as shown in Fig. 16. This diagram only shows vectors of equal length to demonstrate the approximate direction of the flow in order to select the correct orientation. Points that have no vectors are inconclusive.

Once the orientation is known, the data can be postprocessed into velocity and pressure components as shown in Fig. 17. The velocity is nondimensionalized with the freestream velocity, and the static pressure is nondimensionalized with the dynamic pressure. For this final figure the points denoting an out-of-plane velocity were not postprocessed, as this orientation was not measured. For all inconclusive points and out-of-plane points, the velocity and pressure were set equal to zero for the purpose of this figure. Consequently, the pressure and velocity in these areas might appear misleading, at first glance.

At a point the direction might be inconclusive because the flow is unsteady. A point might also be inconclusive because the dynamic pressure is different in the different orientations and that the assumption of a constant dynamic pressure is violated. But, this will only occur if the flow at that point is unsteady. Therefore, for either case an inconclusive point might well be in an unsteady flow. However, if the flow is unsteady then the seven-hole probe is not the appropriate instrument to use. In this way the method presented here also gives us an indication of where data might be questionable and when a different instrument, capable of measuring unsteady flows, should probably be used instead.

VI. Further Discussion

It has already been shown that if the probe tip was in a wake, such that the flow is reversed, then all of the port pressures will read approximately the same value. This has further implications for the use of probes that use a nulling technique, where it is assumed that after nulling ports on opposite sides of a probe, such that they

have the same value, the probe will be facing directly into the flow. However, it is possible that nulling opposite ports could also orient the probe tip away from the flow such that the probe is in a reversed flow. The results obtained from the nulling technique would then be in error.

A possible solution is to ensure that the central hole P_1 is greater than the other holes. But P_1 is also greater than the other holes when the flow is reversed, which implies a knowledge of how much greater P_1 would need to be, or the scale of the recorded probe pressures of the flow. Thus, this is once again the same as estimating the dynamic pressure. Therefore a simple solution to this nulling dilemma is to apply the first rule, as demonstrated earlier.

Estimating the dynamic pressure might not seem like part of an elegant solution. However, the ultimate goal should not be forgotten, that is, to correctly orient the probe toward the flow. Therefore, if the experimenter is in doubt of the direction the probe could be rotated through 180 deg if possible, as was done in the application. The measured pressures in this second position could then be compared directly with those obtained from the first position. Consequently, an improved judgment could be made, using knowledge of the characteristics of the probe found from calibration, as to which direction is correct. This was the approach used for the application given earlier.

The graphs obtained and thresholds set are for the particular probe used in this study. Similar graphs should be obtained for other similar probes, but an examination of this should be carried out at the time of calibration for individual probes. The thresholds, and the amount of rotation, can also be changed depending on the experiment in which the probe is used. For instance, in the case of the second rule presented here a more conservative threshold of 50% could be used. This would exclude angles greater than approximately 40 deg. But if a flow of 45 deg were encountered, a rotation of 90 deg would move the probe through the correct positioning to another incorrect position on the other side. Therefore, with this new more conservative threshold the rotation angle of 90 deg should also be reduced to say 60 deg.

VII. Conclusions

A seven-hole probe with a conical tip was rotated through 360 deg to examine the effect of flow reversal. It was found that rules and procedures could be applied, which made use of the properties of the probe at these high angles, which determined if the probe were incorrectly positioned and consequently if a rotation of the probe were required. The analysis given here highlighted some of the problems that could result from incorrect use of the probe. In particular, the potential to calculate erroneous flow properties exists if the probe is used in regions of very high flow angularity without such an analysis as given here. The Reynolds-number effect of the probe was also briefly examined, and it was found that this effect was greatest within the calibration region at high angles; however, these results are possibly inconclusive because of the short Reynolds-number range tested and the overlap of uncertainty. Regardless, a Reynolds-number effect would not be inhibiting within the calibration region, as stalled ports are not commonly considered when determining flow properties. The methods outlined here also give an indication where the flow might be unsteady and, thus, where a different instrument should be used instead.

Acknowledgments

The authors thank the Australian Research Council and Edmonds Australia Pty., Ltd., for funding this research. The assistance of Simon Davis and Terry Flynn during experimentation is also appreciated.

References

[1]Dominy, R. G., and Hodson, H. P., "An Investigation of Factors Influencing the Calibration of Five-Hole Probes for Three-Dimensional Flow Measurements," *Journal of Turbomachines*, Vol. 115, 1993, pp. 513–519.

[2]Pisasale, A. J., and Ahmed, N. A., "A Novel Method for Extending the Calibration Range of Five-Hole Probe for Highly Three-Dimensional Flows," *Flow Measurement and Instrumentation*, Vol. 13, 2002, pp. 23–30.

[3]Pisasale, A. J., and Ahmed, N. A., "Theoretical Calibration for Highly Three-Dimensional Low-Speed Flows of a Five-Hole Probe," *Measurement Science and Technology*, Vol. 13, No. 7, 2002, pp. 1100–1107.

[4]Everett, K. N., Gerner, A. A., and Durston, D. A., "Seven-Hole Cone Probes for High Angle Flow Measurement: Theory and Calibration," *AIAA Journal*, Vol. 21, No. 7, 1982, pp. 992–998.

[5]Rediniotis, O. K., Hoang, N. T., and Telionis, D. P., "The Seven Hole Probe: Its Calibration and Use," *Instructional Fluid Dynamics Experiments*, FED, Vol. 152, edited by R. S. Budwig, American Society of Mechanical Engineers, New York, 1993, pp. 21–26.

[6]Venkateswara Babu, C., Govardhan, M., and Sitaram, N., "A Method of Calibration of a Seven-Hole Pressure Probe for Measuring Highly Three-Dimensional Flows," *Measurement Science and Technology*, Vol. 9, 1998, pp. 468–476.

[7]Zilliac, G. G., "Modelling, Calibration, and Error Analysis of Seven-Hole Pressure Probes," *Experiments in Fluids*, Vol. 14, 1993, pp. 104–120.

[8]Hoang, N. T., Rediniotis, O. K., and Telionis, D. P., "Hemisphere Cylinder at Incidence at Intermediate to High Reynolds Numbers," *AIAA Journal*, Vol. 37, No. 10, 1999, pp. 1240–1250.

[9]Zilliac, G. G., "Computational/Experimental Study of the Flowfield on a Body of Revolution at Incidence," *AIAA Journal*, Vol. 27, No. 8, 1989, pp. 1008–1016.

[10]Yoon, H. K., and Lilley, D. G., "Further Time-Mean Measurements in Confined Swirling Flows," *AIAA Journal*, Vol. 22, No. 4, 1984, pp. 514, 515.

[11]Rhode, D. L., Lilley, D. G., and McLaughlin, D. K., "Mean Flowfields in Axisymmetric Combustor Geometries with Swirl," *AIAA Journal*, Vol. 21, No. 4, 1983, pp. 593–600.

[12]Rediniotis, O. K., and Kinser, R. E., "Development of a Nearly Omnidirectional Velocity Measurement Pressure Probe," *AIAA Journal*, Vol. 36, No. 10, 1998, pp. 1854–1860.

[13]Treaster, A. L., and Yocum, A. M., "The Calibration and Application of Five-Hole Probes," *ISA Transactions*, Vol. 18, No. 3, 1979, pp. 23–34.

[14]Kline, S. J., and McClintock, F. A., "Describing Uncertainties in Single-Sample Experiments," *International Journal of ASME, Mechanical Engineering*, Vol. 75, 1953, pp. 3–8.

[15]Wenger, C. W., and Devenport, W. J., "Seven-Hole Pressure Probe Calibration Method Utilizing Look-Up Error Tables," *AIAA Journal*, Vol. 37, No. 6, 1999, pp. 675–679.

[16]Johansen, E. S., Rediniotis, O. K., and Jones, G., "The Compressible Calibration of Miniature Multi-Hole Probes," *Journal of Fluids Engineering*, Vol. 123, 2001, pp. 128–138.

[17]Ahmed, N. A., and Archer, R. D., "Performance Improvement of a Bi-Plane with Endplates," *Journal of Aircraft*, Vol. 38, No. 2, 2001, pp. 398–400.

[18]Ahmed, N. A., and Archer, R. D., "Post-Stall Behaviour of a Wing Under Externally Imposed Sound," *Journal of Aircraft*, Vol. 38, No. 5, 2001, pp. 961–963.

[19]Ahmed, N. A., and Archer, R. D., "Testing of a Highly Loaded Horizontal Axis Wind Turbines Designed for Optimum Performance," *International Journal of Renewable Energy*, Vol. 25, No. 4, 2002, pp. 613–618.

R. P. Lucht
Associate Editor